Satellite Gravity Gradiometry: Secular Gravity Field Change over Polar Regions

Philip Moore, Matt A. King

Accepted Manuscript

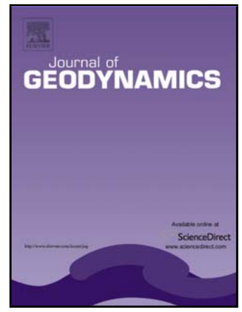

Title: Satellite Gravity Gradiometry: Secular Gravity Field Change over Polar Regions

Authors: Philip Moore, Matt A. King

PII:	S0264-3707(10)00020-7
DOI:	doi:10.1016/j.jog.2010.01.007
Reference:	GEOD 970
To appear in:	*Journal of Geodynamics*
Received date:	25-6-2009
Revised date:	15-12-2009
Accepted date:	6-1-2010

Please cite this article as: Moore, P., King, M.A., Satellite Gravity Gradiometry: Secular Gravity Field Change over Polar Regions, *Journal of Geodynamics* (2008), doi:10.1016/j.jog.2010.01.007

Satellite Gravity Gradiometry: Secular Gravity Field Change over Polar Regions

Philip Moore and Matt A. King
Philip.moore@ncl.ac.uk
School of Civil Engineering and Geosciences, Newcastle University, Newcastle, UK, NE1 7RU

Abstract

The ESA Gravity and steady state Ocean and Circulation Explorer, GOCE, mission will utilise the principle of satellite gravity gradiometry to measure the long to medium wavelengths in the static gravity field. Previous studies have demonstrated the low sensitivity of GOCE to ocean tides and to temporal gravity field variations at the seasonal scale. In this study we investigate the sensitivity of satellite gradiometry missions such as GOCE to secular signals due to ice-mass change observed in Greenland and Antarctica. We show that unaccounted ice mass change signal is likely to increase GOCE-related noise but that the expected present-day polar ice mass change is below the GOCE sensitivity for an 18 month mission. Furthermore, 2-3 orders of magnitude improvement in the gradiometry in future gradiometer missions is necessary to detect ice mass change with sufficient accuracy at the spatial resolution of interest.

Keywords GOCE, gravity field, temporal variations, gradiometry

1. Introduction

Mass redistribution within and on the Earth's surface cause temporal changes to the Earth's gravity field. These temporal signatures are measurable by geodetic techniques including space-borne instrumentation. Over the last decade the scientific community has had access to data from the Gravity Recovery and Climate Experiment (GRACE) mission (Tapley et al., 2004) using precise inter-satellite measurements between a tandem pair of near polar satellites. GRACE has provided the static gravity field to degree and order 100-150 and monthly snapshots of the temporal gravity field for mass redistribution studies. Investigation of these signatures has provided a wealth of knowledge particularly in the areas of hydrology (e.g. Ramillien et al., 2008) and cryospheric science including insight into the changing ice mass over Greenland (e.g. Velicogna et al., 2005) and Antarctica (e.g. Velicogna and Wahr, 2006; Chen et al., 2008).

The ESA Gravity and steady state Ocean and Circulation Explorer, GOCE, mission (Muzi and Allasio, 2004) will utilise the principle of satellite gravity gradiometry to measure the long to medium wavelengths in the static gravity field. While the GRACE mission is based on sensing the differential gravitational forces acting on two point masses orbiting some 220km apart satellite gradiometry carries an array of accelerometers on a single spacecraft to measure the differential accelerations. With GOCE the distance between the point masses, namely the accelerometers, is reduced to 0.5m with the differential accelerations providing the components of the satellite gradient tensor. GOCE was launched into a near polar orbit at an altitude of about 270km on 17 March 2009.

The requirements of the GOCE gradiometry mission have advanced the technological development of satellites. Apart from the highly advanced accelerometers, which are two orders of magnitude more precise than those carried on GRACE, the satellite is a first in both the design of the satellite to ensure a highly stable flight through the Earth's atmosphere and the drag-free control system (e.g. Canuto, 2008) to near-eliminate the effects of the atmosphere. A feedback mechanism from the accelerometers will control firing of ion thrusters to compensate for the drag and other surface force effects. GOCE will carry six accelerometers to measure the gravity gradients along three orthogonal axes. The scientific drivers behind the GOCE mission are described in ESA (1999) for example. Given the band-width limitation of the accelerometers, gradiometry will not be able to measure gravity field signatures at the longest wavelengths. The harmonics causing these long wavelength signatures will instead be recoverable from orbital perturbations utilising precise positioning from the GPS/GLONASS receiver which also provides the necessary orbital positioning. The actual orbit and operational procedure for GOCE will be finalised once in orbit. The pre-launch scenario envisages two six-month measurement phases either side of a six-month period of hibernation during which passage through the Earth's umbra limits power from the solar cells. However, given the low level of solar activity in 2009 other scenarios may be feasible including the potential for continuous measurements over an 18 month period.

Although designed to measure the static gravity field several authors have investigated the sensitivity of the GOCE mission to the temporal field. For example Han et al. (2004), Jarecki et al. (2005) and Han et al. (2006) investigated the effects of the atmosphere, oceans and hydrology in terms of the geoid and gravity gradients.

These studies have shown GOCE to be insensitive to ocean tides and other mass redistributions at the seasonal scale. Others such as Vermeersen (2003) and Vermeersen and Schotman (2008) have investigated the possibility of using GOCE for glacial isostatic adjustment (GIA) studies. In particular, these have identified the possibility of using GOCE measurements to better constrain ice history. In this study we investigate the sensitivity of satellite gradiometry missions such as GOCE to secular ice-mass change observed in Greenland and Antarctica. We utilise rates estimated from the GRACE mission as well as from ERS and ENVISAT radar altimetry and elsewhere. Satellite derived results need to be corrected for GIA for true ice-mass studies but for our purposes it is the total signal over these areas that has been used as the appropriate temporal change affecting space missions. Ice mass loss over Greenland has been observed in several studies and here we use results pertinent to the whole area and to Eastern Greenland which has been shown to be the area of rapid change. Similarly, over West Antarctica the total GRACE mass change is utilised. We also investigate one of the areas of most rapid change in Antarctica namely the Pine Island Glacier with the rates taken from Shepherd et al. (2001).

In practice, the GOCE gradiometry will be accompanied by a non-tidal mass correction computed from an atmospheric and ocean model. In addition the correction will include large scale mass redistribution corrections for the very long wavelengths. These corrections, to be computed from the annual variations of the GRACE spherical harmonic coefficients up to degree and order 20, will effectively account for the ice mass variation within the GOCE gradiometry at spatial scales of 1000km or larger. However, contributions at smaller spatial scales will be excluded from the correction fields. This study is thus motivated by the question to what extent is GOCE or a GOCE satellite gravity gradiometry (SGG) follow-on mission sensitive to ice mass change over Antarctica/Arctic over an 18 months or longer lifetime at long to medium spatial scales.

The study simulates the expected gradiometer signals due to the ice mass change and quantifies the sensitivity in terms of the magnitude of the signal and its spectral power density. In addition, we investigate sensitivity of potential recovery of localized signals over an extended period by using band-width limited windowing functions (Wieczorek and Simons, 2005). By utilising the distinct spatio-temporal spectra of the signal and error (e.g. Han and Simons, 2008; Han and Ditmar, 2008; and Migliaccio et al., 2008) the signal-to-noise ratio over the polar regions can be enhanced. In this study we follow the approach of Han and Simons (2008) and Han and Ditmar (2008) where spatiospectral localization around the epicentre of the 2004 Sumatra-Andaman earthquake facilitated recovery of the geophysical signal even though the signature was unobservable in the original GRACE fields. The methodology takes advantage of the distinct spatiotemporal characteristics of the signal and measurements error to enhance the signal-to-noise ratio of the locally intense signal to the more globally uniform errors in the measurements.

In the final section we consider an idealised future gradiometer mission where the gradiometry is either noise-free or affected by white noise over the band-width of the local signal to investigate potential recovery using 30 day snapshots of data as the mission overflies the Pine Island Glacier.

2. GOCE Gradiometry

The nominal initial GOCE orbit is taken to be at an initial altitude of 270km with semi-major axis of 6648.1363km. The orbit was assumed to be circular with inclination i = 96.65475º. Positioning was computed for a 180 day period with the orbit subject to gravitational effects from the Earth and third bodies. Surface forces were set to zero to mirror the drag-free environment. The altitude of the satellite was seen to oscillate around 265 km. The orbital computations for this period provided the positioning to derive the simulated SGG data. For long-term studies over the lifetime of GOCE the orbit was assumed to repeat after the 6 month hibernation to give a total of 360 days of observations from a 540 day lifetime.

Based on the computed positioning a data set of radial gravity gradients, T_{rr}, was derived at 1 s intervals, the GOCE sampling interval. Noise was subsequently added utilising a characterisation (e.g. Abrikosov and Schwintzer, 2004) of the GOCE power spectral density (PSD) in the radial direction. The noise corresponded to a PSD of 1 mE/√Hz over the measurement band width (MBW) of $5*10^{-3}$ – $1*10^{-1}$ Hz with a PSD proportional to the inverse of the frequency at frequencies below 5*10-3 Hz. The upper frequency is the Nyquist limit of twice the sampling rate. To illustrate the noise threshold on the sensitivity of GOCE gravity field recovery T_{rr} was simulated for the differences between EGM08 (Pavlis et al., 2008) and EGM96 (Lemoine et al., 1998) to degree and order 360. The PSD for this data set is given in Figure 1. Also plotted is the assumed PSD for the gradiometer noise, with the constant value over the MBW. With these noise considerations and altitude near 270km satellite gradiometry cannot determine the longer wavelengths in the gravity field while some shorter-wavelengths are also below the GOCE sensitivity.

3. Secular ice mass change over Greenland.

Ice mass loss from Greenland has been confirmed from both in situ measurements and from GRACE studies. For example Luthcke et al. (2006) employed a mass concentration approach with GRACE data to deduce the rate of change for Greenland divided into six interior regions above 2000m and a further 6 coastal areas below 2000m for July 2003 to July 2005. The interior regions were inferred to have an accumulation of ice of about 40Gton p.a. whilst the coastal areas had a net loss of 140 Gton p.a. East Greenland evidenced the greater loss of ice. The total loss over Greenland of 100 Gton p.a. is considerably less than the ice mass loss of -224±41 Gton from the 2005 mass balance reported by Rignot and Kanagaratnam (2006). On taking the area of Greenland as 1,819,739 km^2 the Rignot and Kanagaratnam value equates to ≈ 0.12m/yr loss in terms of equivalent water height over the entire area. Luthcke et al. (2006) identify South-east and East Greenland (their areas 3b, 4a and 4b) to be the region of high ice loss amounting to 146 Gton per year over an area of 279166 km^2 (see Figure 2). This is equivalent to an ice loss of 0.5 m/yr over the region in equivalent water height. The largest loss of ice per unit area is identified as 75 Gton p.a. in South-East Greenland (their area 3b) of area of about 56109 km^2 equivalent to an ice mass loss of ≈ 1.3m/yr. These rates provide us, in the worst case, with an order of magnitude estimate of likely ice mass change in these regions to be used in our simulations.

To quantify the corresponding impact on the GOCE gradiometry the spatial distribution of the surface ice mass change over the selected area was converted to spherical harmonics rates using the surface load Love number approach of Wahr et al, (1998). Changes from the rates were converted to gravity harmonics up to deg/order 360 at each epoch. These harmonics were subsequently used to generate a global data set of simulated gradiometer observations in the radial direction, T_{rr}, for the mission. The observations can be considered as the temporal change to the static base model. In this analysis it is assumed that the temporal field represents the anomalous potential to be estimated from GOCE.

Figure 3 shows the radial gravity gradient signal of a secular rate of 0.2 m/yr of ice mass over the entire Greenland land mass exhibiting a quasi-secular increase over the two observation periods. For an 18 month period the signal is less than 0.15 mE (1 mE is equivalent to 10^{-12}Gal cm^{-1} or 10^{-12} s^{-2}). The PSD of the radial gradiometry is shown in Figure 4 for the first 30 days and last 30 days of the 18 month period. It shows that the power, with maximum value 1.9 mE/√Hz, is however always below the GOCE measurement noise level of 1 mE/√Hz over the frequency range (Figure 1). Although GOCE is insensitive to the Greenland change it is apparent that neglect of the ice mass loss may increase the PSD noise in the signal to over 1 mE/√Hz at some frequencies.

A similar analysis for an assumed ice mass change of 0.5 m/yr over the area of East and South-East Greenland in Figure 2 is summarised in Figures 5 and 6. The increase in ice mass loss over the area has now yielded a larger signal but the smaller area results in a reduced PSD compared with the whole of Greenland.

Consideration of the gravity gradient signal and the associated PSD gives some insight into the observability but does not necessarily indicate the sensitivity of the gravity field solution to ice mass change. A complementary measure is the degree variance of the gravity field solution in the presence of realistic noise. As the signals originate from a relatively small geographical region it is necessary to localise the signal and noise (Han and Simons, 2008; Han and Ditmar, 2008). In the terminology of Han and Ditmar (2008) the signal is non-stationary while the noise is more likely to be stationary. Techniques of spatiospectral localization (Wieczorek and Simons, 2005) can enhance the signal as the effect decays rapidly outside the region of interest while the measurement errors are relatively uniform over the Earth. Thus, the signal to noise ratio (SNR) of the localized signal is a better measure of the observability of the event. In this way, the 2004 Sumtra-Andaman earthquake was detected by localized analysis of the monthly GRACE gravity field solutions (Han and Simons, 2008). Utilising the localized zonal window function $h(\theta)$ (Eq. 8 of Wieczorek and Simons, 2005) of spherical cap size θ_0 and expanded up to degree $L_h = 2\pi/\theta_0 - 1$ the SNR of the degree variances of the global gravity field solution and the localized solution are presented in Eq. 3-8 of Han and Ditmar (2008). In this study we utilise both the SNR of the signal, where both measurement noise and signal are expanded in spherical harmonics, and the SNR on using a localized window centred on the source of the signal. The spherical harmonic expansion of the measurement noise was taken from Ditmar et al. (2003). The localized SNR is defined for degrees $L_h \leq l \leq L_s\text{-}L_h$ where L_s is the maximum degree of the solution field. For Greenland a spherical cap of θ_0=40° gives $L_h = 8$. Figure 7 shows the SNR for the signal in terms of spherical harmonics and localized by the window function for the ice mass change after 18 months for Greenland and East and South-East Greenland. After application of the spatiospectral localization the SNR has improved but is below unity for all degrees with a maximum SNR of less than 0.3 for all Greenland and 0.25 for East and South East Greenland. Even for a GOCE-like gradiometer an order more accurate than GOCE the signal is only observable for $8 \leq l \leq 18$. A gradiometer three orders more accurate than GOCE will be necessary for recovery of ice-mass change over Greenland within an 18 month mission.

4. Secular ice mass change over Antarctica.

To quantify the signature on GOCE gradiometry from ice mass change over Antarctica we used the secular rates as given by the GRACE mission. Figure 8 is a replot of the figure given in Moore and King (2008) which shows the rate of change of equivalent water height for Aug 2002 – Jan 2006 in mm/yr over Antarctica. This is the spatially averaged mass change and thus includes GIA as well as ice mass rates. The signal over Antarctica is dominated by a negative rate over the West Antarctic Ice Sheet (WAIS), including over Pine Island Glacier. Also evident is an apparent accumulation of mass over the Filchner Ronne Ice Shelf. To investigate the WAIS we have taken an ice mass change of 0.06 m/yr for the region 72°-78°S and 225°-270°E. The corresponding T_{rr} contribution is less than 0.05 mE over the 18month period while the resultant PSD is below the measurement noise by an order of magnitude with a maximum value of ≈ 0.1 mE/√Hz. Equivalently, data from a mission lifetime of a factor of 10 larger than the 18 month assumed here would still just approach the noise level in the MBW. Such a conclusion is not unexpected as the GRACE data underpinning the WAIS analysis is derived from spatial averaging to the extent that the resultant mass change is at large spatial scales whilst satellite gradiometry is more sensitive to medium-short wavelengths in the Earth's gravity field. Analogous to Figure 7 the SNR for WAIS is plotted as Figure 9. For WAIS a spherical cap of θ_0=40 was used. Once again the localized SNR shows an enhancement over the global equivalent but three orders of magnitude below the GOCE measurement sensitivity for degrees $l \geq 40$.

5. Regional Solution

The previous analyses considered the magnitude of the radial gravity gradient and the associated PSD in a sensitivity analysis of ice mass change over Greenland and WAIS on GOCE. In this section, we now contemplate the possibility of an idealised gradiometry mission and seek to recover the observed change in a simulation based on a localized study. For this aspect we have chosen Pine Island Glacier in the WAIS. Pine Island Glacier is one of the areas of most rapid change in Antarctica. Figure 10, replotted from Shepherd et al. (2001), shows the measured rate of change of ice as inferred from ERS altimetry (1992-1999). As an extreme characterisation of potential ice mass change the area of 23660km^2 bounded by 74.5ºS - 76ºS and 261ºE - 266ºE was considered to be experiencing a change of 0.5m/yr of ice. As for the whole Antarctica study a set of radial gravity gradient measurements were simulated and the PSD deduced. Although the maximum Trr signal after 18 months of 0.1 mE is a factor of two larger than for the WAIS the PSD is lower than that of the WAIS with a maximum value of 3.10^{-2} mE/√Hz.. The sensitivity of gradiometry to shorter wavelengths is however evident in the less rapid reduction in the PSD amplitudes with signatures close to the maximum being measured at frequencies from 10^{-3} Hz to 10^{-2}

Hz. The SNR for Pine Island is plotted in Figure 9. The rapid ice-mass change is evident in the increased sensitivity compared to WAIS at degrees $l \geq 30$.

Given the regional nature of the analysis a localized base function methodology based on that proposed by Ilk et al. (2003) and Mayer-Gürr et al. (2005, 2006) is adopted. Accordingly, the anomalous potential, T, at satellite point position r, is represented as

$$T = \sum_{i=1}^{I_{\max}} \alpha_i \Phi(r, r_{Q_i})$$

where r_{Q_i} is the surface point corresponding to node Q_i , I_{max} the total number of nodes and α_i the coefficients to be estimated from the gradiometry. The localized base function Φ is given by

$$\Phi(r, r_{Q_i}) = \frac{GM}{R_e} \sum_{n=1}^{N_{\max}} k_n \left(\frac{R_e}{r} \right)^{n+1} P_n(\cos\psi_{r, r_{Q_i}})$$

where G is Newton's gravitational constant, M the mass of the Earth of radius R_e, P_n the Legendre polynomial of degree n, $\psi_{r,r_{Q_i}}$ the geocentric angle between the satellite position and the ith surface node Q_i ($\vec{r}_{Q_i}$) and

$$k_n = \sum_{m=0}^{n} \Delta C_{l,m}^2 + \Delta S_{l,m}^2$$

the expected covariances of degree n based on the covariances $\Delta C_{l,m}^2, \Delta S_{l,m}^2$ in the spherical harmonics. Rather than risk possible aliasing due to tuning the covariances to the expected signal we utilised general values for k_n taken from the differences between EGM08 and EGM96. Figure 11 shows that the local base functions rapidly decay to zero with geocentric angle.

For the localized analysis the nodes were restricted to latitudes 60ºS to 90ºS. The nodes were spaced on N_{lat}=60 circles of latitude formed using N_{tri} = 5 equal triangles with common apex at the South Pole, each spanning 72º of longitude. Over each triangle a total of j nodes were equally distributed along the jth circle of latitude counting away from the pole. The total number of nodes was thus I_{max}=N_{tri} * N_{lat}*(N_{lat}+1)/2. Of these nodes those between 84ºS and 90ºS were removed given the polar gap due to the GOCE inclination. With *Imax*= 9150 this left a total of 8760 nodes and coefficients α_i to be estimated. A subset of the nodes across Antarctica and Pine Island Glacier is shown as Figure 12. The simulated T_{rr} data was taken for separate 30 day periods utililising short arcs across the pole of ≈16min duration. Each 30 day period involved 84265 from 518400 observations in the global set. In the analysis the data was assumed to be noise free with no restriction due to band-width whilst the satellite positioning was assumed exact. The application of white-noise at a level significantly below the PSD across the band-width of the measurements will lead to similar results. Thus, it is assumed that coloured noise as seen with GOCE is not significant in any future gradiometer mission. At the GOCE altitude the maximum Trr over the 18 months never exceeded 0.1 mE whist the PSD was always below 0.04 mE/√Hz. In practice, a gradiometer with reduction in noise by 2-3 orders of magnitude compared with GOCE is necessary. To illustrate the enhancement due to a decrease in altitude an alternative data set at initial altitude of 230km (mean altitude 225km) was derived. The radial gravity gradients for the two altitudes are shown in

Figure 13 for the final month of the 18 month time span considered in the study. The decrease from 265 to 235 km in mean altitude effectively doubles the magnitude of the largest signal.

The true geoid height rates for the Pine Island Glacier are plotted as Figure 14a. There is some spatial distortion of the constant signal over the area 74.5ºS - 76ºS and 261º-266ºE due to the restriction to degree and order 360 in the gravity field. The maximum rate of change is 2.89 mm over the 18 months. Figures 14b and 14c plot the corresponding rates for the regional solution from gradiometry at mean altitude of 265 km (max change 2.70 mm) and 225 km (max 3.06 mm) respectively. Note that as the effective rates corresponded to the midpoint of month 17 the rates were multiplied by 18/17.5 for consistency with Figure 14a. The lower altitude is preferable in terms of gravity field recovery but the higher altitude also supports recovery to a high level. The analysis shows that the local base function approach is capable of measuring changes over a region such as Pine Island Glacier and that gradiometry can, in theory, support solutions recovered from 30 days of data as for GRACE.

6. Conclusions:

Studies across Arctic/Antarctic establish insensitivity of GOCE to ice mass change at nominal noise PSD over the expected 18 month lifetime. In fact only a uniform ice-mass change of 0.2m across all of Greenland approached the GOCE noise PSD. Areas of greatest ice mass change such as East and South-East Greenland and Pine Island Glacier in the West Antarctica ice shelf are too small spatially with signatures orders of magnitude below the GOCE noise PSD. Thus, observed rates of ice mass change will have negligible impact on static gravity field recovery from GOCE. Alternatively, for the WAIS, a mission lifetime of a factor of 10 larger than the 18 month assumed for GOCE would still yield signals less than the noise level in the MBW. This was expected as the GRACE signal that underpinned the WAIS analysis was derived using spatial averaging with the resultant mass change at a relatively large spatial scale. Satellite gradiometry is more sensitive to medium-short wavelengths in the Earth's gravity field.

The use of localized windowing enhances the ice mass change signal as the effect decays rapidly outside the region of interest while the measurement errors are relatively uniform over the Earth. This methodology has been shown to increase the signal-to-noise ratio of the effects of ice-mass change but the recovery signal is still 2-3 orders of magnitude below the GOCE sensitivity in the MBW.

Analysis of data over Pine Island Glacier utilising a local base function methodology demonstrated the potential of gradiometry for temporal gravity field studies. The results showed that in the idealised case of error free gradiometry without any band-width limitations the local base function approach was capable of recovering the expected change over areas such as Pine Island Glacier (23660 km^2). In practice, this would require a future SGG mission some 3 orders of magnitude more precise than GOCE.

Acknowledgments

The authors which to thank the UK Natural Environment Research Council for financial support and the two anonymous reviewers for their constructive comments and suggestions.

References:

Abrikosov, O., Schwintzer, P., 2004, Recovery of the Earth's gravity field from GOCE satellite gravity gradiometry: A case study, in Proc. Second International GOCE User Workshop, *"GOCE, the geoid and Oceanography"*, Frascati, Italy, 8-10 March 2004, ESA SP-569.

Canuto, E., 2008, Drag-free and attitude control for the GOCE satellite, Automatica, 44**,** 1653-1932.

Chen, J.L., Wilson, C.R., Tapley, B.D., Blankenship, D.D., Young, D., 2008, Antarctic regional ice loss rates from GRACE, Earth and Planetary Science Letters, 266, 140-148.

Ditmar, P., Kusche, J., and Klees, R., 2003. Computation of spherical harmonic coefficients from satellite gravity gradiometry data: regularization issues. J. Geo.,,, 77, 465-477.

ESA, 1999, Gravity Field and Steady-State Ocean Circulation Mission, ESA SP-1233.

ESA-ESRIN, 2004, Proc. Second International GOCE User Workshop, "GOCE, the geoid and Oceanography", Frascati, Italy, 8-10 March 2004, ESA SP-569.

Han, S.C., Shum, C.K., Ditmar, P., Braun, A., Kuo1, C., 2004, Effect of High-Frequency Temporal Aliasing on GOCE Gravity Field Solution, Proc. Second International GOCE User Workshop "GOCE, The Geoid and Oceanography".

Han, S.-C., Shum, C.K., Ditmar, P., Visser, P., van Beelen, C., Schrama, E.J.O., 2006, Aliasing effect of high-frequency mass variations on GOCE recovery of the Earth's gravity field, J. Geodyn., 41, 69-76.

Han, S.-C., Ditmar, P., 2008, Localized spectral analysis of global satellite gravityfields for recovering time-variable mass redistributions, J. Geod., 82, 423-430.

Han, S.-C., Simons, F.J., 2008, Spatiospectral localization of global geopotential fields from GRACE reveals the coseismic gravity change due to the 2004 Sumatra-Andaman earthquake, J. Geophy. Res., 113, B01405.

Ilk, K.H., Feuchtinger, M., Mayer-Gürr, T., 2003, Gravity Field Recovery and Validation by Analysis of Short Arcs of a Satellite-to-Satellite Tracking Experiment as CHAMP and GRACE, In: F. Sansò (ed.) A Window on the Future of Geodesy, IUGG General Assembly 2003, Sapporo, Japan, International Association of Geodesy Symposia, Vol. 128, pp. 189-194, Springer,

Jarecki, F., Müller, J., Petrovic, S., Schwintzer, P., 2005, Temporal gravity variations in GOCE gradiometric data - In: C. Jekeli, C.; Bastos, L.; .Fernandes, J. (Eds.), Gravity, geoid and space missions : GGSM 2004 ; IAG International Symposium Porto, Portogal ; August 30 - September 3, 2004, Springer, 333-338.

Lemoine, F.G., Kenyon, S.C., Factor, J.K., Trimmer, R.G., Pavlis, N.K., Chinn, D.S., Cox, C.M., Klosko, S.M., Luthcke, S.B., Torrence, M.H., Wang, Y.M., Williamson, R.G., Pavlis, E.C., Rapp, R.H., Olson, T.R., 1998, The Development of the Joint NASA GSFC and the NIMA Geopotential Model EGM96, NASA/TP-1998-206861.

Luthcke, S.B., Rowlands, D.D., Lemoine, F.G., Klosko, S.M., Chinn, D, McCarthy J.J., 2006, Monthly spherical harmonic gravity field solutions determined from

GRACE inter-satellite range-rate data alone, Geophys. Res. Lett., 33, L02402, doi:10.1029/2005GL024846.

Mayer-Gürr, T., Ilk, K.H., Eicker, A., and Feuchtinger, M., 2005, ITG-CHAMP01: a CHAMP gravity field model from short kinematic arcs over one-year observation period, J. Geod., 78, 462-480.

Mayer-Gürr, T., Eicker, A., and Ilk, K.H., 2006, In: Flury, J., Rummel, R., Reigber, C., Rothacher, M., Boedecker, G., Schreiber, U., Observation of the Earth System from Space, Springer Berlin Heidelberg, 131-148.

Migliaccio, F., Reguzzoni, M., Sansò, F., Dalla Via, G., Sabadini, R. 2008. Detecting geophysical signals in gravity satellite missions. Geophys. J. Int., 172, 56-66.

Moore, P., King, M.A., 2008. Antarctic ice mass balance estimates from GRACE: Tidal aliasing effects. Journal of Geophysical Research-Earth Surface, 113, F02005, doi:10.1029/2007JF000871.

Muzi D., Allasio A., 2004, GOCE: the first core Earth explorer of ESA's Earth observation programme, Acta Astronautica, 54, 167-175.

Pavlis, N,K., Holmes, S.A., Kenyon, S.C., Factor, J.K., 2008, An Earth Gravitational Model to degree 2160: EGM2008. Presented at the 2008 General Assembly of the European Geosciences Union, Vienna, Austria, April 13-18, 2008.

Ramillien, G., Bouhours, S., Lombard, A., Cazenave, A., Flechtner, F., Schmidt, R., 2008, Land water storage contribution to sea level from GRACE geoid data over 2003–2006, Glob. Planet. Change **60** (3–4), 381-392.

Rignot, E., Kanagaratnam, P., 2006, Changes in the velocity structure of the Greenland ice sheet. Science, **311**, 986–990.

Shepherd, A.J., Wingham, D.J., Mansley, J. A.D., Corr, H.F.J., 2001, Inland Thinning of Pine Island Glacier, West Antarctica, Science 2, 291,862-864.

Tapley, B.D., Bettadpur, S., Watkins, M., Reigber, C., 2004, The gravity recovery and climate experiment: Mission overview and early results, Geophys. Res. Lett., 31, No.L09607, 10.1029/2004GL019920.

Velicogna, I., Wahr, J., Hanna, E., and Huybrechts, P., 2005, Short term mass variability in Greenland, from GRACE, Geophys. Res. Lett., 32, L05501, doi:10.1029/2004GL021948.

Velicogna, I., Wahr, J., 2006, Measurements of time-variable gravity show mass loss in Antarctica, Science, 10.1126/science.1123785.

Vermeersen, L.L.A., 2003, The potential of GOCE in constraining the structure of the crust and lithosphere from post-glacial rebound, Space Sci. Rev. 108 (1–2), 105–113.

Vermeersen, L.L.A., Schotman, H.H., 2008. High-harmonic geoid signatures related to glacial isostatic adjustment and their detectability by GOCE. J. Geodyn. 46, 174–181.

Wahr, J., Molenaar, M., and Bryan, F., 1998, Time-Variability of the Earth's Gravity Field: Hydrological and Oceanic Effects and Their Possible Detection Using GRACE, J. Geophys. Res., 103, 30205-30230.

Wieczorek, M. A., Simons, F.J., 2005, Localized spectral analysis on the sphere, Geophys. J. Int., 162, 655-675, doi:10.1111/j.1365-246X.2005.02687.x.

Figure Captions

Figure 1: Power spectral density of the differences between EGM08 and EGM96 to degree and order 360. The black line shows the adopted noise threshold.

Figure 2. 1° x 1° latitude/longitude block diagram of Greenland (grey), showing the East and South East regions (black).

Figure 3. Radial gravity gradient signal over a 540 day period resulting from 0.2 m/yr ice mass change over Greenland.

Figure 4. PSD of radial gravity gradient signal resulting from 0.2 m/yr ice mass change over Greenland. Days 0-30 (grey) and 510-540 (black).

Figure 5. Radial gravity gradient signal resulting from 0.5 m/yr ice mass change over East and South-East Greenland.

Figure 6. PSD of radial gravity gradient signal resulting from 0.5 m/yr ice mass change over East and South-East Greenland. Days 0-30 (grey) and 510-540 (black).

Figure 7. GOCE degree variance signal-to-noise ratio (SNR). Global spherical harmonics: Greenland (circles) and SE Greenland (crosses). Localized harmonics (Lh): Greenland (solid line) and SE Greenland (stippled line).

Figure 8. Mass change rates in mm/yr of equivalent water heights for the period 2002-2006 estimated from GRACE (replotted from Moore and King, 2008).

Figure 9. GOCE degree variance signal-to-noise ratio (SNR). Global spherical harmonics: Western Antarctic Ice shelf (WAIS) (circles) and Pine Island (PI) (crosses). Localized harmonics (Lh): WAIS (solid line) and PI (stippled line).

Figure 10. The rate of elevation change of the lower 200 km of Pine Island Glacier between 1992 and 1999 (coloured scale) registered with a map of the ice surface

speed (gray scale) from Shepherd et al. (2001). Reprinted with permission from AAAS.

Figure 11. Normalised local base function

Figure 12. Distribution of nodes across Antarctica with Pine Island Glacier shaded grey.

Figure 13. Simulated Pine Island Glacier radial gravity gradiometry signal from mission at 230 km (black) and 270km (red).

Figure 14. Change in geoid height (mm) over 18 months. Top: (a) true signal (max 2.89 mm); middle: (b) regional solution from gradiometry at 265 km (max 2.70 mm); lower: (c) regional solution from gradiometry at 225 km (max 3.06 mm).

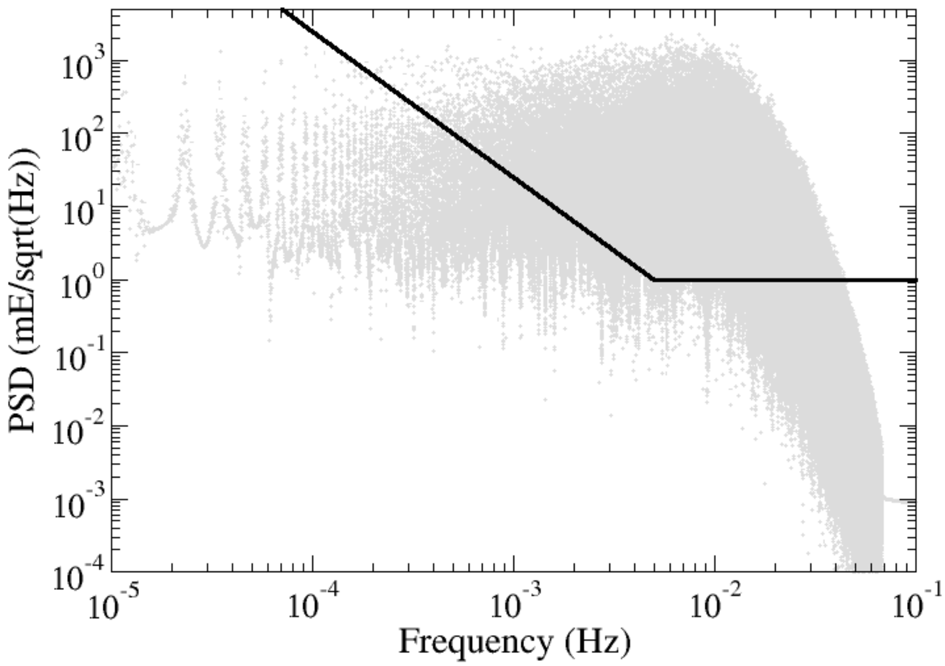

Figure 1: Power spectral density of the differences between EGM08 and EGM96 to degree and order 360. The black line shows the adopted noise threshold.

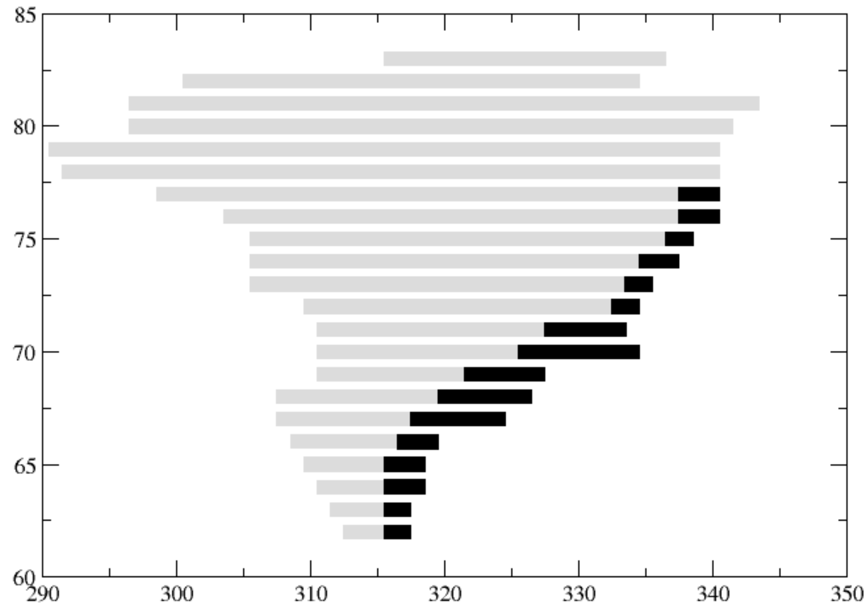

Figure 2. 1° x 1° latitude/longitude block diagram of Greenland (grey), showing the East and South East regions (black).

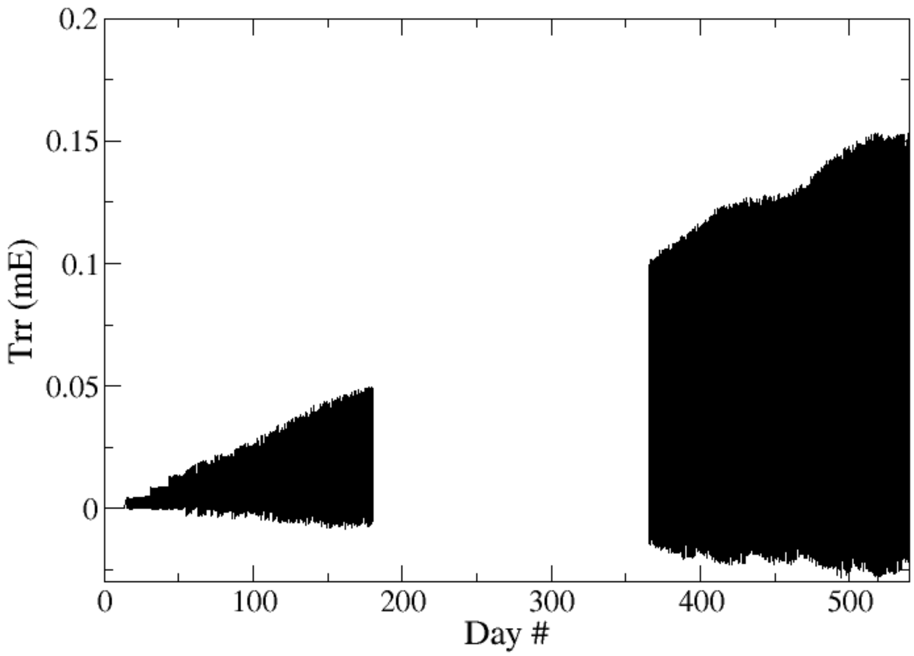

Figure 3. Radial gravity gradient signal resulting from 0.2 m/yr ice mass change over Greenland.

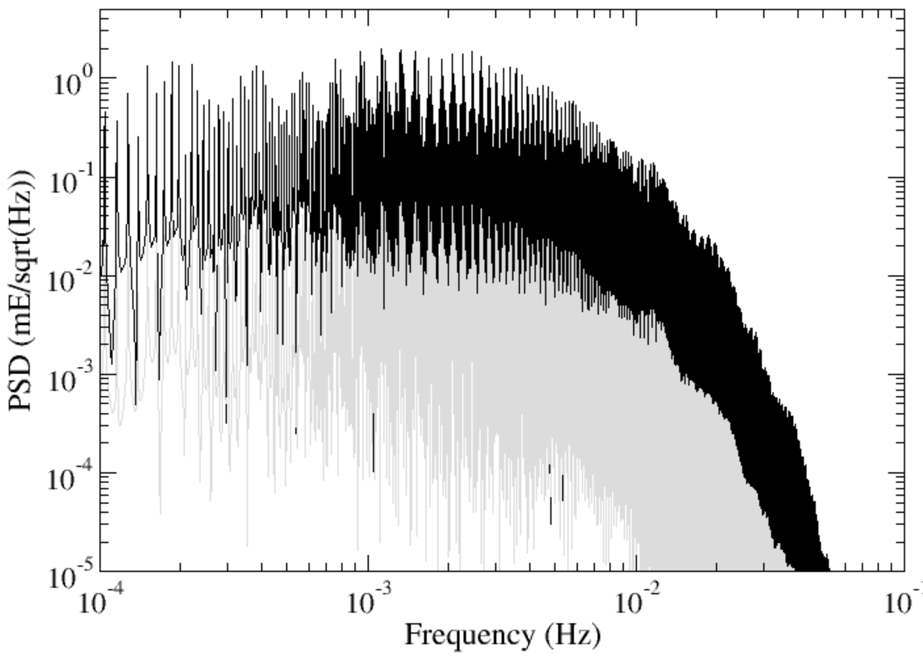

Figure 4. PSD of radial gravity gradient signal resulting from 0.2 m/yr ice mass change over Greenland. Days 0-30 (grey) and 510-540 (black).

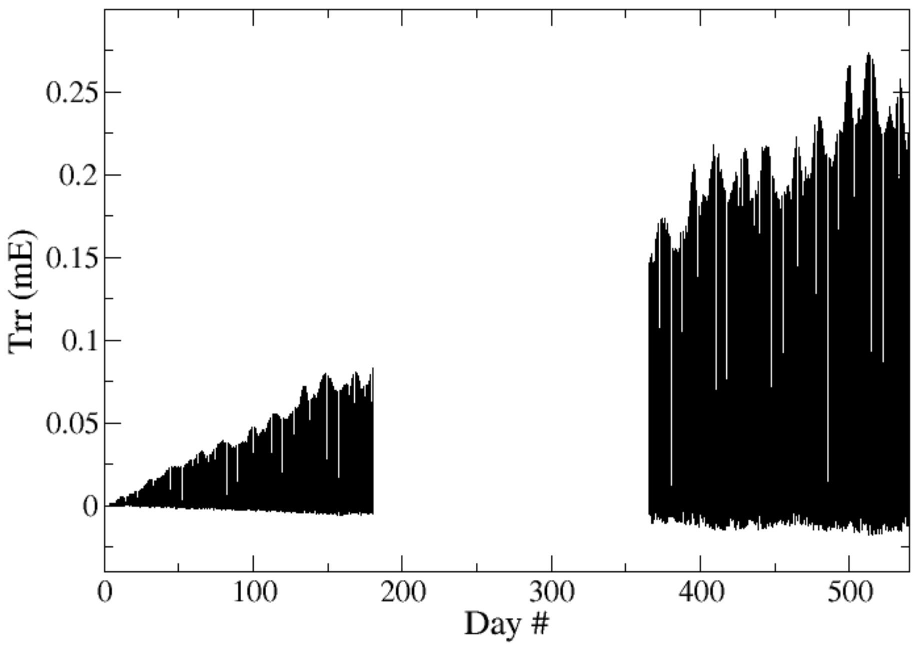

Figure 5. Radial gravity gradient signal resulting from 0.5 m/yr ice mass change over East and South-East Greenland.

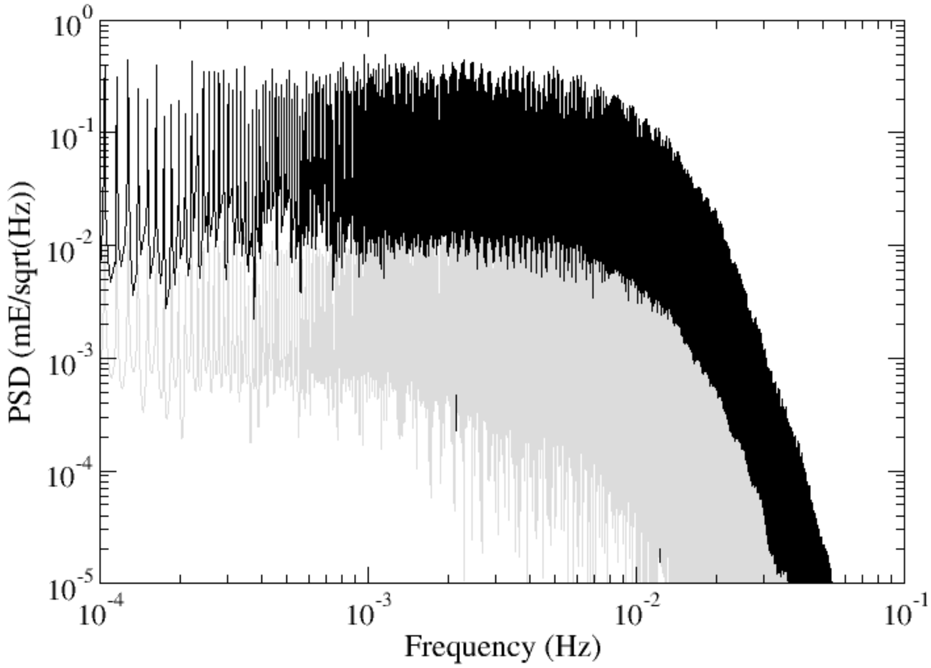

Figure 6. PSD of radial gravity gradient signal resulting from 0.5 m/yr ice mass change over East and South-East Greenland. Days 0-30 (grey) and 510-540 (black).

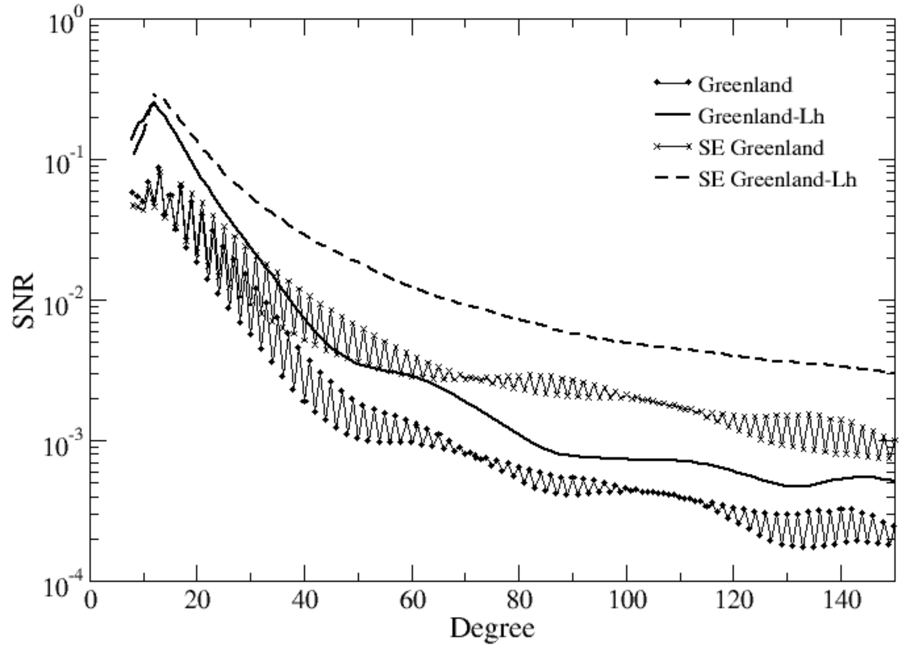

Figure 7. GOCE degree variance signal-to-noise ratio (SNR). Global spherical harmonics: Greenland (circles) and SE Greenland (crosses). Localised harmonics (Lh): Greenland (solid line) and SE Greenland (stippled line).

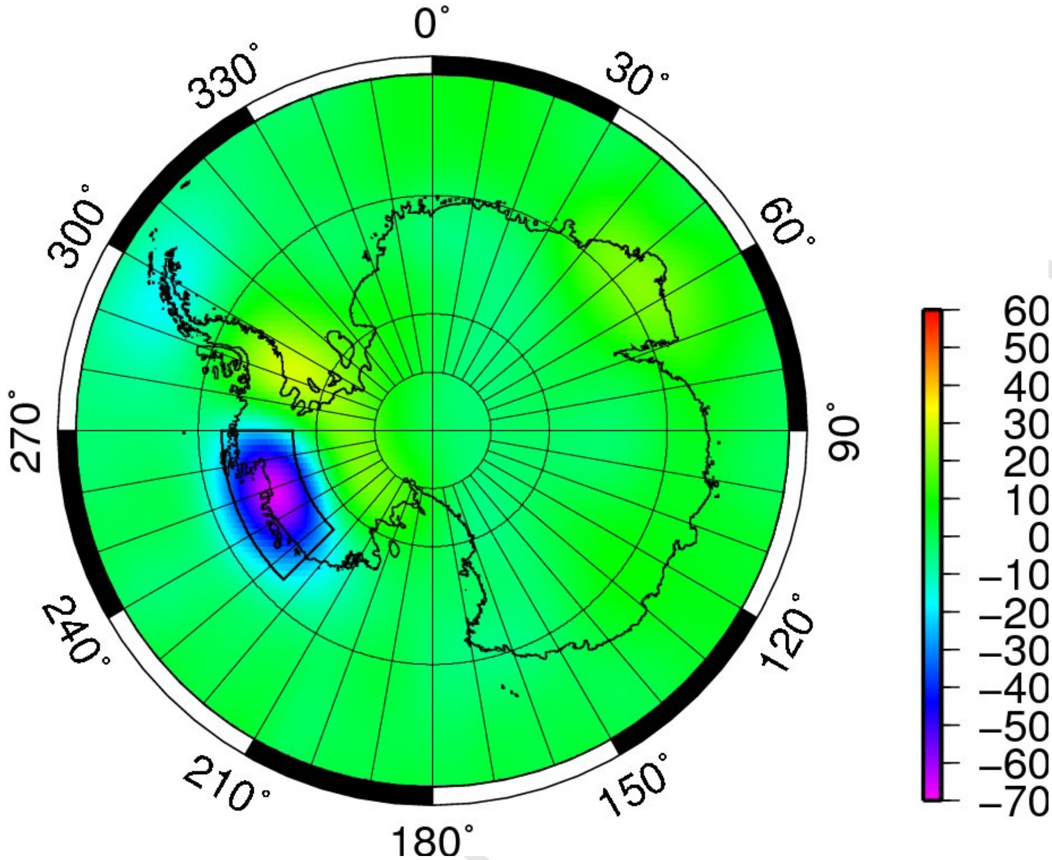

Figure 8. Mass change rates in mm/yr of equivalent water heights for the period 2002-2006 estimated from GRACE (replotted from Moore and King, 2008).

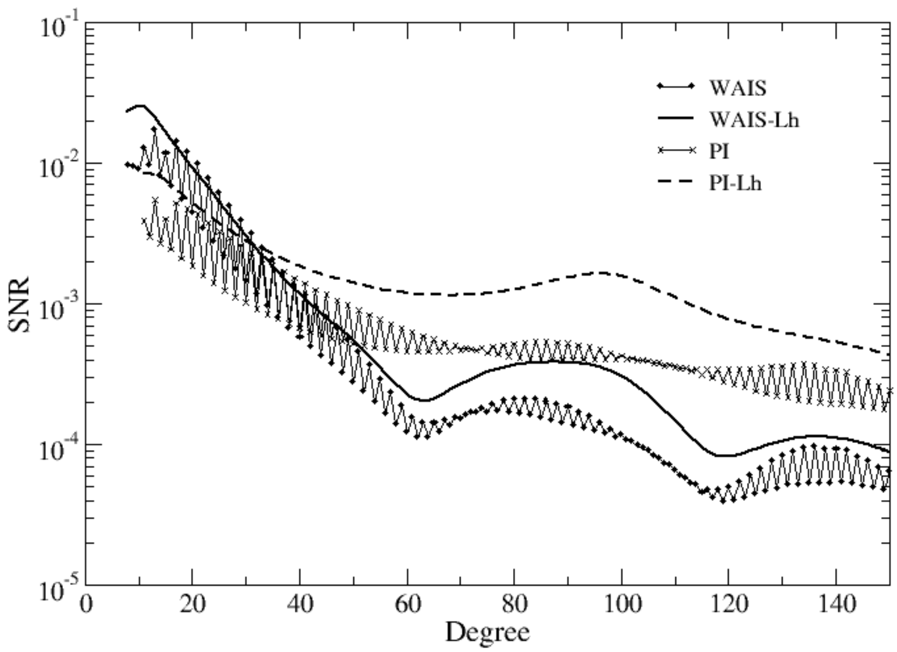

Figure 9. GOCE degree variance signal-to-noise ratio (SNR). Global spherical harmonics: Western Antarctic Ice shelf (WAIS) (circles) and Pine Island (PI) (crosses). Localised harmonics (Lh): WAIS (solid line) and PI (stippled line).

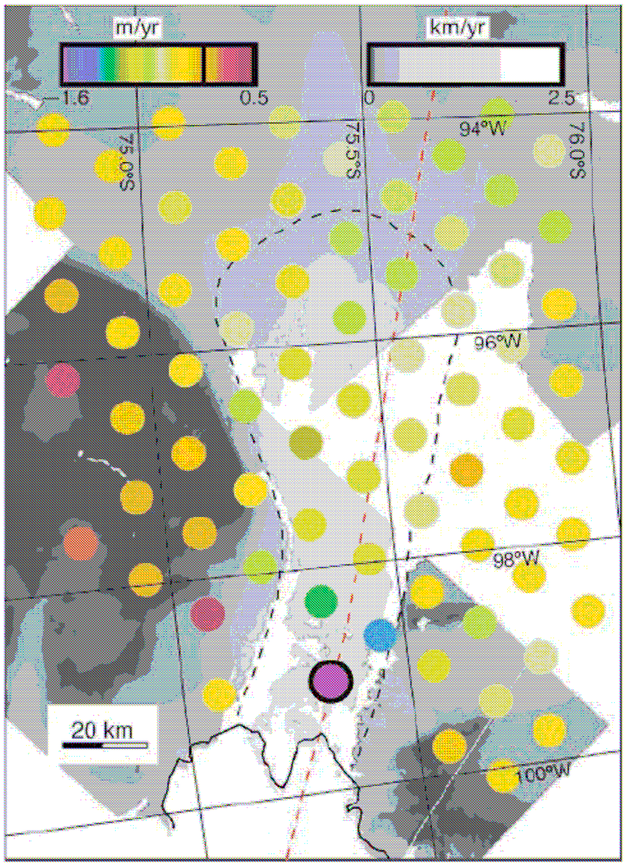

Figure 10. The rate of elevation change of the lower 200 km of Pine Island Glacier between 1992 and 1999 (coloured scale) registered with a map of the ice surface speed (gray scale) from Shepherd et al. (2001). Reprinted with permission from AAAS.

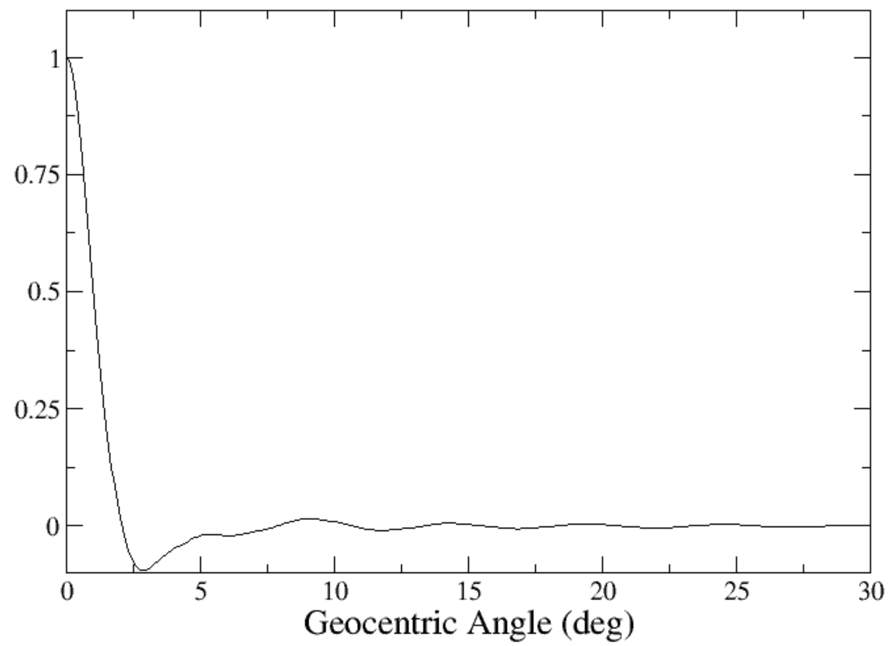

Figure 11. Normalised local base function.

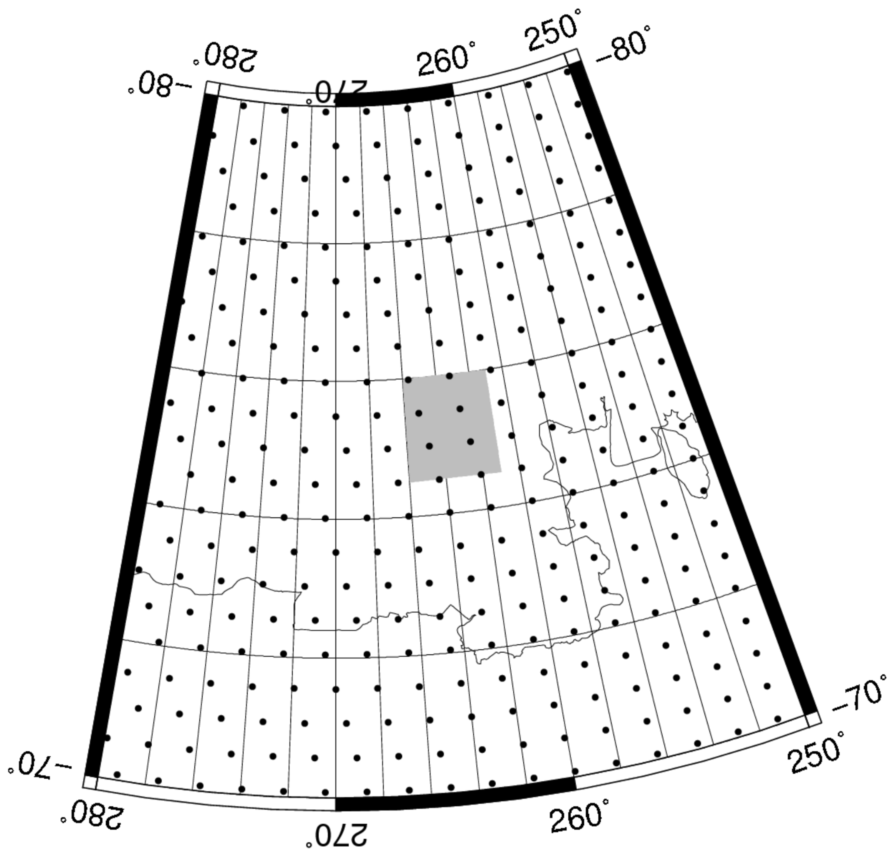

Figure 12. Distribution of nodes across Antarctica with Pine Island Glacier shaded grey.

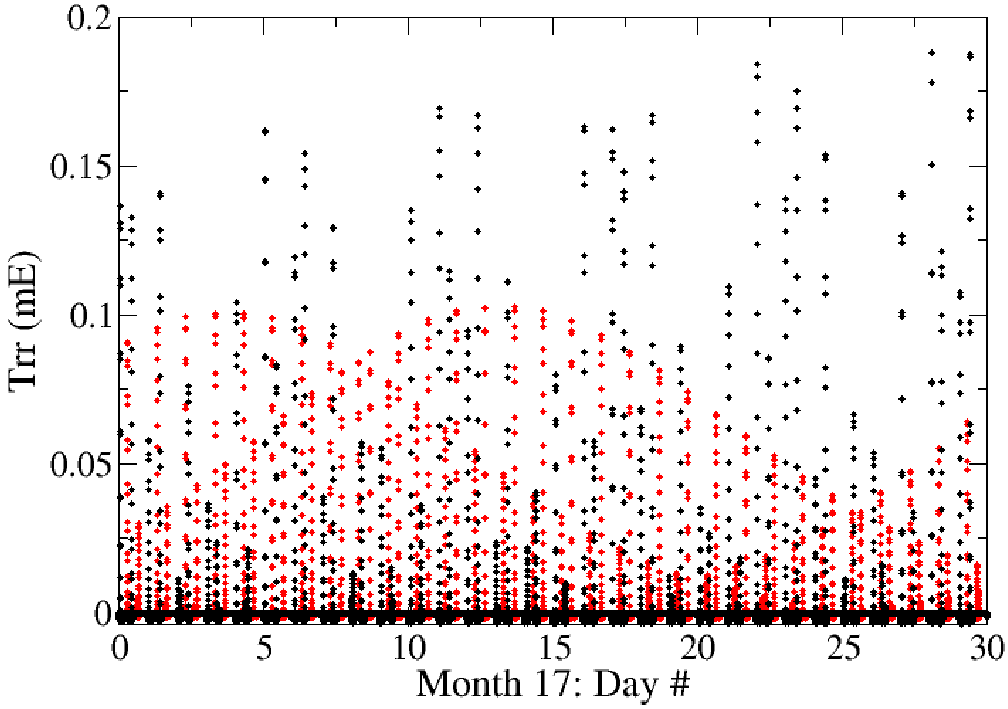

Figure 13. Simulated Pine Island Glacier radial gravity gradiometry signal from mission at 230 km (black) and 270km (red).

(a)

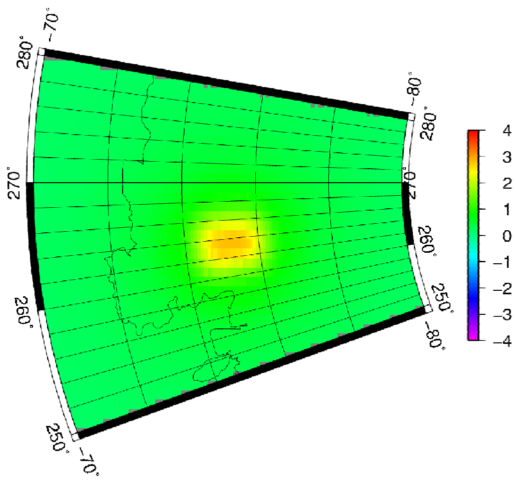
-70°
280°
-80°
280°
270°
270°
260°
250°
260°
-80°
250°
-70°
4
3
2
1
0
−1
−2
−3
−4

(b)

(c)

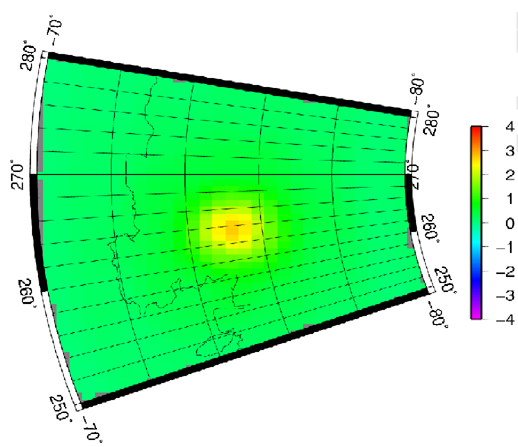
-70°
280°
-80°
280°
270°
270°
260°
250°
260°
-80°
250°
-70°
4
3
2
1
0
−1
−2
−3
−4

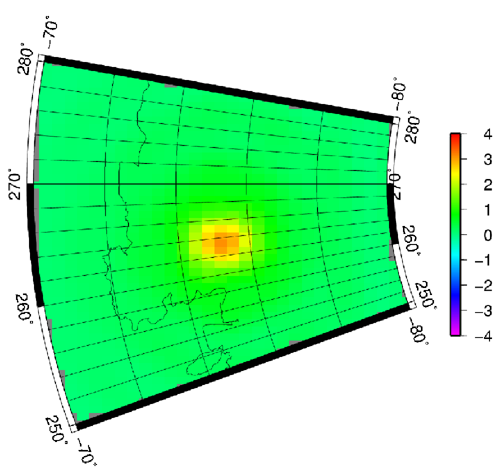
-70°
280°
-80°
280°
270°
270°
260°
250°
260°
-80°
250°
-70°
4
3
2
1
0
−1
−2
−3
−4

•

Figure 14. Change in geoid height (mm) over 18 months. Top: (a) true signal (max 2.89 mm); middle: (b) regional solution from gradiometry at 265 km (max 2.70 mm); lower: (c) regional solution from gradiometry at 225 km (max 3.06 mm).